A. E. YOUSIF

Liquid-Solid Lubricants in Conditions Pertinent to Isothermal Elastohydrodynamic Line Contact Lubrication

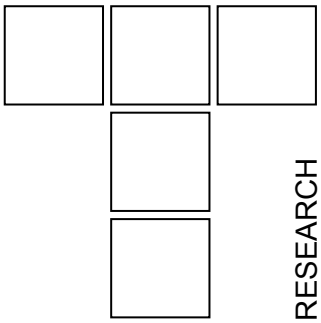

A study of the isothermal elastohydrodynamic (EHL) line contact problem lubricated with deforming and degrading non-newtonian liquid-solid systems is presented. Oil with solid particle additives undergoes stress induced deformation and degradation of the solid particles. The effective lubricant viscosity experiences reversible and irreversible losses. The reversible loss of the effective lubricant viscosity (shear thinning) is due to non-newtonian rheology of the fluid and variations in the fluid shear rate, and high pressure gradient. The irreversible loss of the effective lubricant viscosity is caused by the deformation and degradation processes of the solid additives dispersed in the lubricant. Thus, the lubricant viscosity in the contact zone experiences reversible and irreversible losses and, in general is a discontinuous function. The changes in lubricant viscosity alter virtually all parameters of the lubricated contact such as film thickness and shape, friction stresses, and pressure. The type, shape, size, and concentration of additive particles dispersed in the oil must be considered. A generalized Reynolds equation for liquid-solid system was solved numerically for weight fraction and pressure distribution. The use of liquid-solid lubricants enhanced the load capacity and reduced the coefficient of friction between the moving surfaces. Attenuation in the spikes of the pressure distribution curves near the outlet of the contact zone was obtained which may be responsible for reducing the occurrence of pitting in the rolling surfaces. Frictional traction-slip curves showed lower traction coefficiensts than those for pure oil. This makes their use undesirable in applications of high traction drives.

Key words: *two-phase lubricants, liquid-solid lubricants, elastohydrodynamics.*

1. INTRODUCTION

Non-newtonian behavior in lubricating oils is attributed to the solid additives used, such as, graphite and MoS_2. These additives are dispersed in the oil in the form of powders and carried by the oil to form a liquid-solid lubricant. They reduce friction and wear by interposing a thin adherent layer of material that shears easily and prevent direct contact between the rubbing surfaces.
The aim of this study is to characterize the behavior of the liquid-solid lubricants in isothermal E.H.L. line contact. The shape, size, and concentration of solid particles will form basic study requirements.

Albert E. Yousif
College of Engineering, Nahrain University, Baghdad-Iraq
Presently visiting professor, College of Engineering, Cairo University, Cairo-Egypt

2.THEORETICAL CONSIDERATIONS

The viscosity of the liquid-solid lubricant may be affected by the dispersion of the solid particles. Such solids act as thickening agents. The Einstein equation, [1] is a good approximation for the relation between the viscosity of the suspension and the concentration of the solid particles. The equation can be written as:

$$\eta = \eta_o (1 + 2.5C) \tag{1}$$

where C <<1,volumetric concentration of solid additives; η_o viscosity of liquid alone which is a function of temperature, pressure and mixture, and η is the mixture viscosity. In the present work C was replaced by a^3, postulated by:

$$a^3 = 1/[1 - (1 - 1/\lambda)\rho_p / \rho_o] \tag{2}$$

where, λ is the percentage of particles by weight, ρ_p and ρ_o are the densities of solid particles and oil

respectively. The modified viscosity expression was used with the new generalized Reynolds equation for mixtures, [2].

1. Lubricant model

The configuration of the two rolling cylinders in E.H.L line contact with the (liquid-solid) lubricant is shown in Fig.1. The particle is given the shape of ellipsoid which can mathematically be modified into a sphere and a rod-like particle. The following assumptions are made in the development of the governing equations:

1. Infinitely long cylinders.
2. The viscosity of the liquid-solid varies with pressure, and with particle concentration.
3. The density of the mixture varies with pressure and with the solid weight fraction.
4. The ellipsoidal particles have a size of the order or slightly larger than the film thickness.
5. Uniform distance between any two adjacent particles within the conjunction.

1.2. Governing equations

Assuming both the fluid and solid phases are continuous (each point within the mixture is accompanied by fluid and solid constituents together at each position) from continuum mechanics point of view, so that the properties of the mixture may be represented by a continuous function of position. The mass distribution of the particles in the mixture is a continuous function of position, λ(x) where ($0 \le \lambda \le 1$), is the solid weight fraction defined as the ratio of the weight of particles to the weight of the mixture at a point in the mixed region, where "a point" should be considered as "a point and its neighborhood". Therefore, specification of λ at a point implies an average of the solid weight fraction in the neighborhood of that point. Similarly, all other physical quantities associated with the point are averaged in the same sense over the neighborhood with center is at the specified position. The density of the mixture at a given point is dependent upon the weight percentage of the solid particles content. Therefore, a new density equation to combine the effect of the two densities will be as follows:

$$\rho_m = \rho(1-v) + \rho_p v \qquad (3)$$

where ν, is the volume fraction of the solids (Q_p/Q)

Thus,

$$\rho_m = \{\rho_o(1+0.6p)/(1+1.7\mathrm{p})\}(1-\lambda)(\rho/\rho_p) + \rho_p\lambda(\rho/\rho_p) \qquad (4)$$

The first term in the right hand side of the last equation is similar to that introduced by Dowson and Higginson, [3], except it is multiplied by (1-λ) which represents the fluid weight percent. The second term stands for the density of the solid phase multiplied by the solid weight percent. In terms of the weight percentage ratio, λ for the solid particles dispersion in the two-phase lubricant is:

$$\lambda = Q_p\rho_p/[Q_p\rho_p + Q_f\rho]$$

Now since, $$Q = Q_p + Q_f \qquad (5)$$

Then, $$\lambda = Q_p\rho_p/[Q_f\ \rho_m] \qquad (6)$$

Therefore, $$\lambda = v/[v + 1(1-v)\rho/\rho_p] \qquad (7)$$

The volume of every solid particle is taken as "ellipsoid". The shapes considered in the present analysis have one axis of symmetry, see Fig. (2). Let D and d be the diameters of the ellipsoid in the x and y direction respectively. The volume of ellipsoid (A) is $(\frac{\pi}{6})Dd^2$, and the volume of ellipsoid (B) is $\left(\frac{\pi}{6}\right)D^2d$. As a result the number of particles entering the conjunction in unit time and width for the two ellipsoid models (A and B) should take into account the occupancy of these particles within the carrier fluid in which they disperse. Thus, the two equations for models A and B respectively are:

$$n = \frac{6}{\pi d^2 D} Uh_c(\rho/\rho_p)/[1-\lambda(1-\rho/\rho_p)] \qquad (8)$$

and $$n = \frac{6}{\pi D^2 d} Uh_c(\rho/\rho_p)/[1-\lambda(1-\rho/\rho_p)] \qquad (9)$$

since the side leakage is ignored then:

$$Q = \int_{y=0}^{h} udy = Uh_c \qquad (10)$$

where h_c is the film thickness at $(dp/dx) = 0$.

Now, denoting $\nu = \dfrac{\forall_m}{\eta_x \forall_p}$, then equation (7) becomes

$$\lambda = 1\Big/\left[1-\left(\frac{\forall_m}{\eta_x\forall_p}-1\right)\frac{\rho}{\rho_p}\right] \qquad (11)$$

where $\forall_m$ and $\forall_p$ are the volumes of mixture and solid particles. Now, for a liquid-solid lubricant the Reynolds equation takes the following form, [4]:

$$\frac{d}{dx}\left\{\frac{h^3}{6}\frac{\partial p}{\partial x} - Uh\left[\left(1-\frac{1}{1+\left(\frac{\forall_m}{n_x\forall_p}-1\right)\frac{\rho}{\rho_p}}\right)\eta + \frac{1}{1+\left(\frac{\forall_m}{n_x\forall_p}-1\right)\frac{\rho}{\rho_p}}\eta_s^o\right]\right\} = 0 \qquad (12)$$

1.3. The elastic and plastic deformation of particles and bounding surfaces

When the dispersed solid particles in pure oil come in the conjunction they may suffer considerable elastic or plastic deformations. Under elastic conditions, the deformation of the solid particles and that of the lubricated surfaces must be taken into account. Fig. (3) shows an ellipsoidal particle that is elastically deformed between two parallel surfaces. Let v, v_p, E, and E_p be the Poisson's ratios and the elastic modulii of the rolling surfaces and the particles material respectively. Then the elastic deformation of the solid particles within the conjunction may be written as follows:

$$\left(\frac{1-v_1^2}{\pi E_1}+\frac{1-v_2^2}{\pi E_2}\right)\frac{q_o\pi^2}{4a}(2a^2-\breve{r}^2)=\delta-\frac{R_1+R_2}{2R_1R_2}\breve{r}^2 \quad (13a)$$

where,
$$\delta=\left(\frac{1-v_1^2}{\pi E_1}+\frac{1-v_2^2}{\pi E_2}\right)\frac{q_o\pi^2}{2a} \quad (13b)$$

$$a=\left(\frac{1-v_1^2}{\pi E_1}+\frac{1-v_2^2}{\pi E_2}\right)\frac{q_o\pi^2(R_1+R_2)}{4a(R_1R_2)} \quad (13c)$$

$$q_o=\frac{3W_i}{2\pi a^2} \quad (13d)$$

$$\frac{d-h_i}{2}=\left[\frac{9}{16}\frac{W_i^2}{\Re}\left(\frac{1-v_1^2}{\pi E_1}+\frac{1-v_2^2}{\pi E_2}\right)\right]^{1/3} \quad (13e)$$

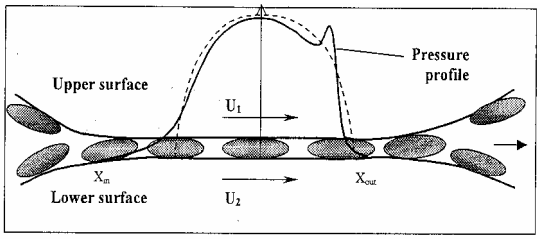

Figure 1. E.H.L. line contact configuration with liquid-solid lubricant containing ellipsoidal particles.

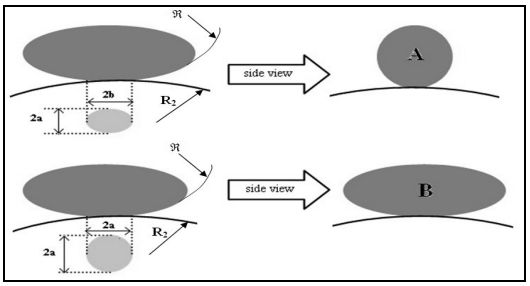

Figure 2. Two ellipsoidal particle models

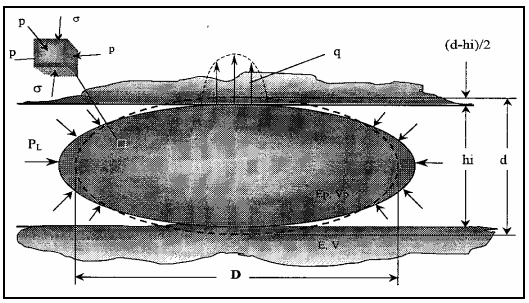

Figure 3. An ellipsoidal particle deformed elastically.

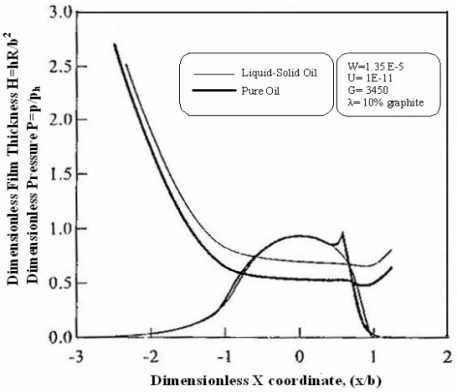

Figure 4. Pressure distribution and film shape showing the comparison between the pure oil and the liquid-solid lubricant

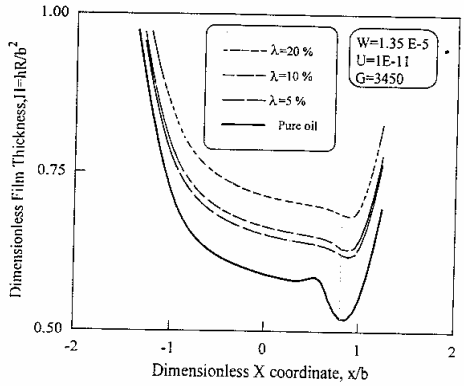

Figure 5. Film shape showing the effect of increasing the dispersion of MoS_2 solid particles (the film nip tends to move outwards)

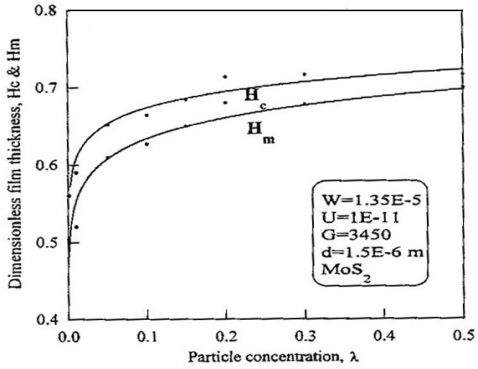

Figure 6. Effect of particle concentration on central film thickness for MoS_2.

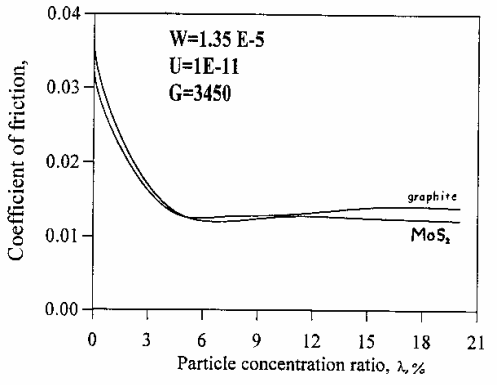

Figure 7. The effect of particle concentration on the coefficient of friction for MoS_2 and graphite.

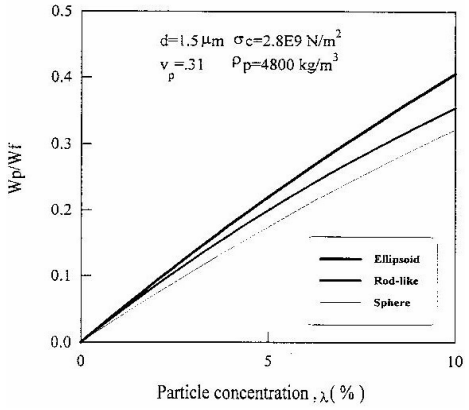

Figure 8. Particle shapes effect on load capacity ratio for particle of MoS_2.

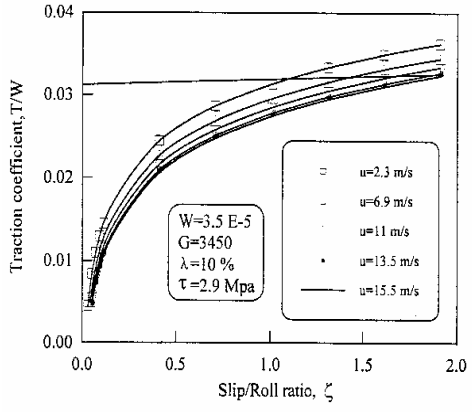

Figure 9. Traction coefficient as a function of slip ratio for liquid-solid lubricant (MoS_2) at various rolling speeds.

where δ is the deformation of the two bodies, r is a position between $(0 \rightarrow a)$, a is the radius of the contact area, and q_o is the pressure intensity at contact. The radius R_2 is treated as an infinite number.

Also, d is the diameter of the particle in y-direction, and □ is the radius of curvature of the particle which is easily computed. Solving equation (15e) for the load capacity contributed by an individual particle,

$$W_i = \frac{\sqrt{2}}{3}(d-h)^{3/2}\sqrt{\Re}\Big/\left(\frac{1-\nu_p^2}{E_p}+\frac{1-\nu^2}{E}\right) \quad (14)$$

$$A_i = \pi\left[\frac{3}{4}W_i\Re\left(\frac{1-\nu_p^2}{E_p}+\frac{1-\nu^2}{E}\right)^{3/2}\right] \quad (15)$$

where A_i is the contact area between the particle and the bounding surfaces.

For a spherical particle equation (15) reduces to:

$$W_i = \frac{1}{3}(d-h)^{3/2}\sqrt{d}\Big/\left(\frac{(1-\nu^2 p)}{E_p}+\frac{(1-\nu^2)}{E}\right) \quad (16)$$

Equation (16) is applicable only when the area of contact is a circular one. For other types of particles, the contact area must be obtained by knowing the contact area geometry of the particle.

1.4. Load carrying capacity

The total load supported by the solid particles is:

$$W_p = \sum_{j=1}^{n_z}\sum_{i=1}^{n_x} W_{ij} \quad (17)$$

Where W_{ij} is the load supported by an individual particle; n_x and n_z are numbers of particles in the x and z directions respectively. Thus, the numbers of particles flowing into the contact zone per unit time and per unit width in the x and z directions are:

$$n_x = L_x\sqrt{\frac{6\lambda}{\pi d^3}h_c\left(\frac{\rho}{\rho_p}\right)}\Big/\left[1-\lambda\left(1-\frac{\rho}{\rho_p}\right)\right] \quad (18)$$

and, $$n_z = L_z\sqrt{\frac{6\lambda}{\pi d^3}h_c\left(\frac{\rho}{\rho_p}\right)}\Big/\left[1-\lambda\left(1-\frac{\rho}{\rho_p}\right)\right] \quad (19)$$

Now, for every infinitesimal column in x-direction, the load in the z-direction supported by the particles is the same. Then equation (17) becomes:

$$W_p = n_z\sum_{i=1}^{n_x} W_i \quad (20)$$

The total load capacity due to the hydrodynamic action and due to the particles is:

$$W_T = W_F + W_P \quad (21)$$

W_F can be computed from:

$$W_F = L_z\int_{x_{in}}^{x_{out}} p\,\mathrm{d}x \quad (22)$$

1.5. Volumetric flow rate

Under steady-state conditions, the statements of conservation of mass for the fluid and solid constituents may be written as follows:

$$\frac{\partial}{\partial x}\left[(1-\lambda)u_x\right]+\frac{\partial}{\partial y}\left[(1-\lambda)u_y\right] \quad \text{for fluid} \qquad (23)$$

$$\frac{\partial}{\partial x}\left(\lambda \mathrm{v}_x\right)+\frac{\partial}{\partial y}\left(\lambda \mathrm{v}_y\right)=0 \qquad \text{for solid} \qquad (24)$$

Integration of the above equations between the limits 0 and h, using Leibnitz's general integration rule results in the following equations:

$$Q=\int_o^{h(x)}(1-\lambda)u_x \mathrm{d}y \qquad (25)$$

$$\text{and} \quad M_s=\int_o^{h(x)}\lambda v_x \mathrm{d}y \qquad (26)$$

where Q is the mass flow rate of the fluid phase, and M_s is that for the solid phase.

1.6. Shear stress in the mixed flow

The two constituents of oil and solid exist in one cell in order to represent the shear stress components The normal and shear stress of the mixture, τ_{yy}, and τ_{xy} are: $\tau_{yy}=-p$, and

$$\tau_{xy}=\frac{2y-h(x)}{2}\frac{\partial \mathrm{p}}{\partial x}-\frac{U\Gamma(x)}{h(x)}+\frac{\eta_s^o\lambda}{h(x)}\left[B_2(x)+U-B_1(x)\right] \qquad (27)$$

Evaluating equation (27) at $y = 0$, we get:

$$\tau_{\mathrm{xy}}\,|_{\mathrm{y}=0}=\frac{-1}{h(x)}\left\{\frac{h^2(x)}{2}\frac{\partial p}{\partial x}+U\Gamma(x)=\eta_s^o\lambda\left[B_2(x)+U-B_1(x)\right]\right\} \qquad (28)$$

Equation (28) can be used to calculate the frictional traction coefficient of the mixture flow as:

$$f=\frac{F_x}{W} \qquad (29)$$

where F_x and W are the friction force and the load capacity of the mixture flow which can be written as follows: $F_x=\int_o^L \tau_{xy}\,|_{y=0}\,\mathrm{d}x$, and $W=\int_0^{\mathrm{L}} p\,\mathrm{d}x$

If no slip condition is assumed between the particles and boundaries then $B_1=U$ and $B_2=0$ we get:

$$u_x=\frac{1}{\Gamma(x)}\left\{\frac{y^2-h(x)y}{2}+\frac{\lambda(\eta_s^o)^2}{\theta^2\Gamma(x)}\left[1-\frac{e^{\theta\lambda(x)y}}{1+e^{\theta\lambda(x)h(x)}}-\frac{e^{\theta\lambda(x)y}}{1+e^{-\theta\lambda(x)h(x)}}\right]\right\}\frac{dp}{dx}+U\left[1-\frac{y}{h(x)}\right] \qquad (30)$$

$$u_x=u_y=\frac{1}{\Gamma(x)}\left\{\frac{y^2-h(x)y}{2}+\frac{\lambda(\eta_s^o)^2}{\theta^2\Gamma(x)}\left[1-\frac{e^{\theta\lambda(x)y}}{1+e^{\theta\lambda(x)h(x)}}-\frac{e^{\theta\lambda(x)y}}{1+e^{-\theta\lambda(x)h(x)}}\right]\right\}\frac{dp}{dx}+U\left[1-\frac{y}{h(x)}\right] \qquad (31)$$

$$\frac{\partial}{\partial x}\left[\frac{h^3(x)}{6}\frac{\partial_p}{\partial x}-Uh(x)\Gamma(\mathrm{x})\right]=0 \qquad (32)$$

$$\frac{\partial}{\partial x}\left\{\frac{1}{\Gamma(x)}\left[\frac{h^3(x)}{6}+\frac{2\eta_s^o\left(\eta_s^o-\eta\right)\lambda(1-\lambda)\psi_1(x)}{\Gamma(x)\,\theta^2}\right]\frac{\partial p}{\partial x}-Uh(x)\right\}=0 \qquad (33)$$

$$\tau_{\mathrm{xy}}\,|_{\mathrm{y}=0}=\frac{-1}{h(x)}\left[\frac{h^2(x)}{2}\frac{\partial p}{\partial x}+U\Gamma(x)\right] \qquad (34)$$

The total stress in the mixture flow, using the scales for the material functions and noting that $\lambda=\lambda(x)$, can be written as, [4]

$$T=-p\begin{bmatrix}1 & 0\\ 0 & 1\end{bmatrix}+\begin{bmatrix}0 & \eta(1-\lambda)\frac{\partial u_x}{\partial y}+\lambda\eta_s^o\frac{v_x}{\partial y}\\ \eta(1-\lambda)\frac{\partial u_x}{\partial y}+\lambda\eta_s^o\frac{v_x}{\partial y} & 0\end{bmatrix} \qquad (35)$$

2. NUMERICAL SOLUTION FOR THE MIXTURE

The generalized Reynolds equation (12) in the absence of particle slippage at the boundaries was integrated, discretized, and solved by the finite difference method. For an assumed pressure distribution (Hertzian), as an initial evaluation, the equation was solved for the weight solid fraction distribution. Once the value of λ is available, then equation (12) is solved for pressure distribution. This equation is a partial differential one and is solved using successive over-relaxation method. The values of pressures and their gradients are then used to update the weight fraction distribution. The cycle is repeated until the solution of both λ and p converged. The relative error between two successive iterations fell between a specified tolerance (0.002-0.005).

3. RESULTS AND DISCUSSION

The dimensionless parameters used in the EHL calculations are defined in the computer program. These are: material parameter $G=\alpha\hat{E}$; load parameter $W=\frac{W}{ER}$; speed parameter H=h/R; and pressure parameter $P=p/p_H$. The properties of the oil and the rollers materials, [5] are shown in Table (1). The properties of the solid particles materials are as shown in Table (2), [6].

Table 1. Properties of the oil and cylinders, [5]

Viscosity SAE 30 (at 50˚C), η_o	Density of the oil ρ	Viscosity-pressure coeff. of the oil, α	Elastic modulus of the cylinders E	Equivalent radius of the cylinders R
0.04 Pa.s	850 kg/m^3	1.6 E-8 (m^2/N)	2.3 E11 (N/m^2)	0.04 m

Table 2. Properties of solid lubricants, [6]

Solid lubricant	E_p(N/m^2)	Comp. St. (N/m^2)	ρ_p (kg/m^3)	ν_p
MoS_2	3.2 E10	2.8 E9	4800	0.31
Carbon graphite	2.7 E10	2.8 E8	1730	0.3

The film thickness increases progressively with increasing particle concentration ratio, see Fig. (4).

For low concentration the pressure profiles for the lubricants tend to develop rounded spikes. These spikes disappear at concentration above 5% for both types of solids. This adds an advantage to the use of liquid-solid lubricant by reducing the probability of pitting of the metal rolling surfaces and in addition, it may improve the fatigue limit to some extent. As a result, the pressure distribution will have a slightly different profile with a cut off side in the exit direction. This is in agreement with the work of Kodnir *et al*, [7], see Fig. (5). The nip near the exit decreases gradually with increasing solid weight concentration for both types of solid particles. The nips have a tendency to move towards the exit side.

All pressure and film shape curves were plotted with an error falling in the range (0.00135-0.0043). The central and minimum film thickness, Fig. (6) was plotted against various solid weight concentrations. The two plots showed a non-linear (logarithmic increase). The present work results were fitted for a wide range of solid weight concentration λ=(5-50)%. The minimum film thickness for both liquid solid lubricants as follows:

$$H_{\mathrm{m}}|_{\mathrm{liquid-solid}} = H_{\mathrm{m}}|_{\mathrm{oil}} + [0.02\ln\lambda + 0.2] \text{ graphite} \quad (34)$$

$$H_{\mathrm{m}}|_{\mathrm{liquid-solid}} = H_{\mathrm{m}}|_{\mathrm{oil}} + [0.03\ln\lambda + 0.2] \quad MoS_2 \quad (35)$$

The variation of the friction coefficient with solid concentration for both lubricants is shown in Fig. (7). The friction coefficient decreases gradually up to a constant minimum value of (5-7%), with increasing weight concentration ratios. The dispersed articles tend to crowd near the center of contact (close to the point of dp/dx=0). For the conditions given in the figure the distribution ratio (λ/λ_o) has a value of 1.6, meaning that more than one-half of the inlet particles are crowded at the middle of the contact. Fig. (8), shows the effect of particle shapes and concentrations on the load carrying capacity for MoS_2. It is clearly seen that the ellipsoidal and rod-like particles give a higher load than the spherical particles. Fig. (9), shows a typical traction-slip curve for various rolling speeds.

4. CONCLUSIONS

1. The liquid-solid lubricant provided higher film thickness than the liquid lubricant, especially with the ellipsoidal particles. This enhancement in film thickness showed a non-linear relation with particle concentration. There exists an optimal concentration of approximately 7%.
2. The friction coefficient of the liquid-solid lubricant was less than that with pure oil alone.
3. The spikes of the pressure profile vanished progressively with increasing solid percentage.
4. The load capacity is largely affected by the size of the dispersed solid particles. However, this effect is limited to the value of (d=1.5h_c) after which the loads tend to remain constant.
5. No benefit was sensed in using shapes of aspect ratios (D/d=2). This ratio serves as an optimum aspect ratio for the ellipsoidal shaped particles, The rod-like and ellipsoidal particles gave better load capacity than the spherical particles.
6. The traction-slip curves indicated that lubricants with suspended solid particles present lower traction coefficients than pure lubricants.

REFERENCES

[1]. A. Einstein: "Berichting Zu Meiner Arbeit: Eine Neue Bestimmu Der Molekudimensionen", Annalen der Physik, Vol. 34, pp. 591-592, 1911.

[2]. M.M. Khonsari, F. Dai: Generalized Reynolds Equation for Solid-Liquid Lubricated Bearings, ASME Journal of Applied Mechanics, Vol. 61, pp. 460-466.

[3]. D. Dowson, G.R. Higginson: Elasto-hydrodynamic Lubrication, 2nd edition, Pergamon Press, Oxford, 1977.

[4]. M.M. Khonsari, F. Dai: Analytical Solution for a Mixture of a Newtonian Fluid and Granules in Hydrodynamic Bearings, Wear, Vol. 156, pp. 327-344, 1992.

[5]. A.E. Yousif: The Tribological Characteristics of Lubricating Greases in Heavily Loaded Contacts, PIS, Gearing and Power Transmissions, Vol.1, Tokyo, Japan, 1981.

[6]. F.J. Clauss: Solid Lubricants and Self Lubricating Solids, Academic Press, New York, 1972.

[7]. D. S. Kodnir, R.G. Salukvadze, D.L. Bakashivilli, V.Sh. Shwartman: A Solution of the Elasto-hydrodynamic Problem for non-Newtonian Fluids, ASME Journal of Lubrication Technology, Vol. 97, No.2, pp. 303-320, 1975.